**Supplemental Figure 1**

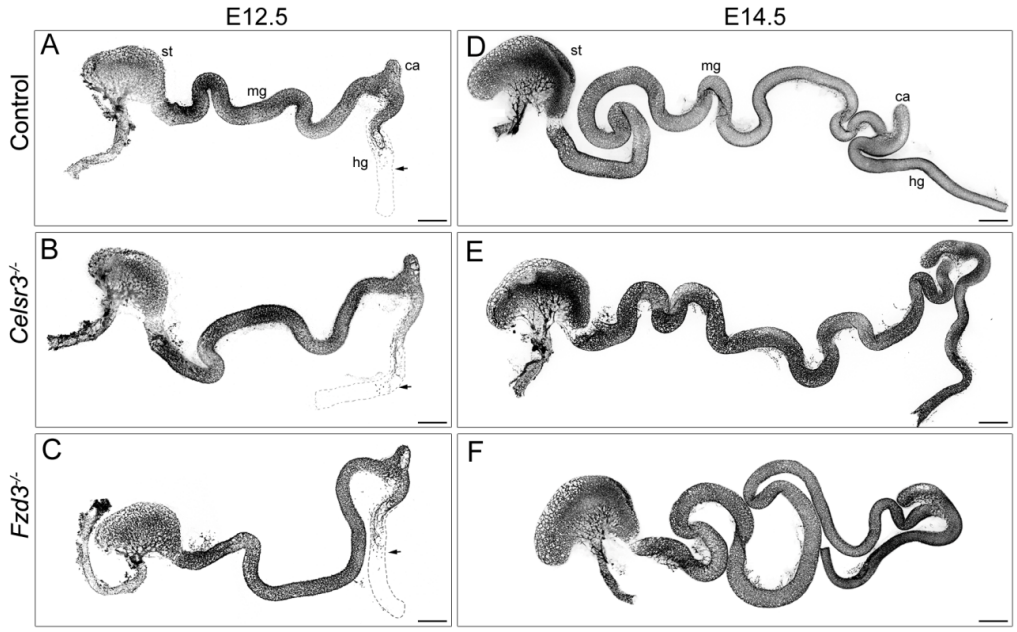


Deletion of *Celsr3* and *Fzd3* does not affect the colonization of the gut by enteric neural crest cells. GFP immunostaining of whole mount gut preparations from E12.5 (**A** to **C**) and E14.5 (D to F) *Wnt1-Cre;R26R-EYFP* embryos that were either wild-type (A and D), *Celsr3*$^{-/-}$ (B and E) or *Fzd3*$^{-/-}$ (C and F). Arrows indicate the extent of colonization of the E12.5 guts by GFP$^{+}$ cells. At E14.5, all guts irrespective of genotype were fully colonized. Ca, caecum; hg, hindgut; mg, midgut; st, stomach. Scale bars, 500 µm.

**Supplemental Figure 2**

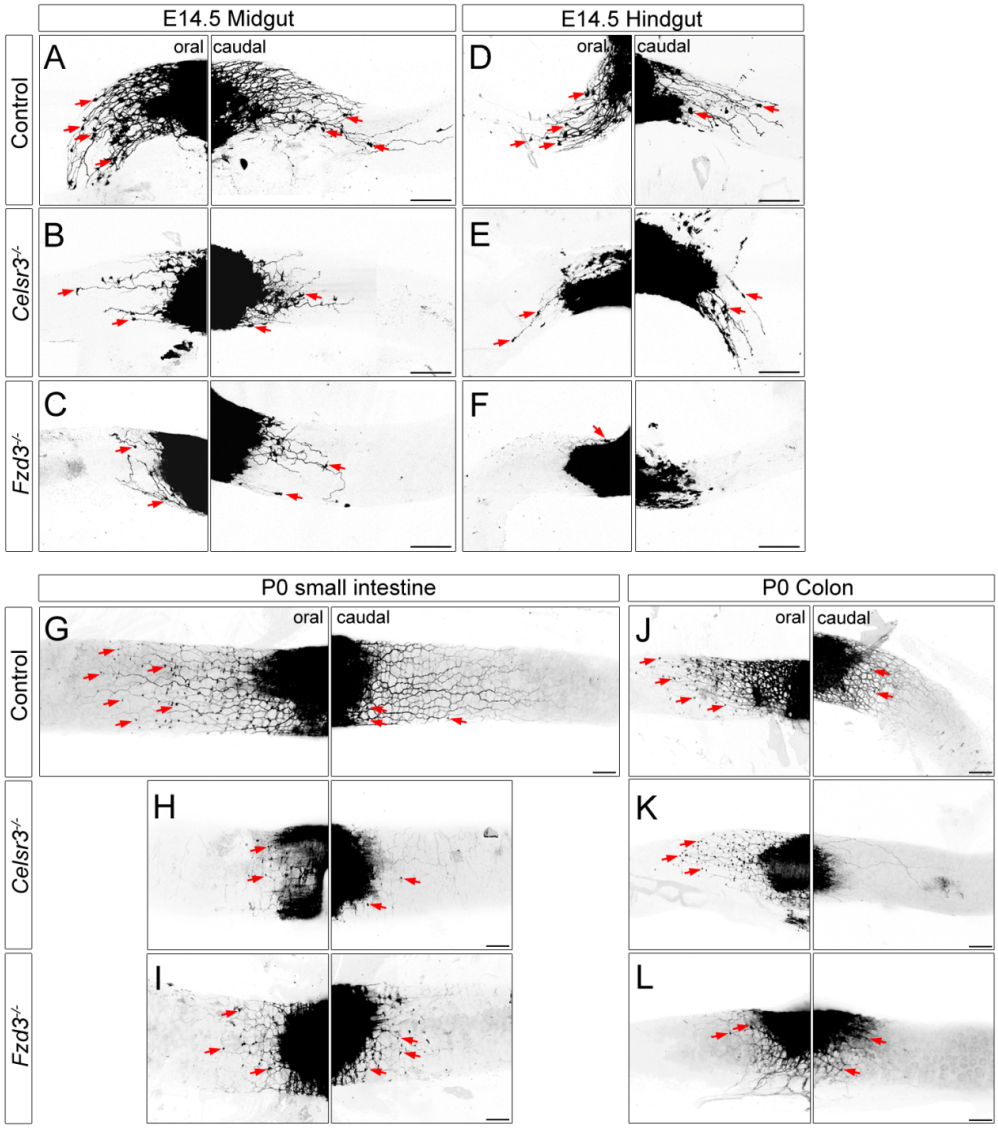


Defects in the organization of the enteric neuronal plexus are observed throughout embryogenesis. Focal application of DiI in the midgut (A to C) and hindgut (D to F) of E14.5 embryos, and the small intestine (G to I) and colon (J to L) of P0 pups of the indicated genotypes. Note the severe reduction in the number and length of labeled projections and in the number of labeled cell bodies (arrows) in the gut of Celsr3 and Fzd3 mutants. Grayscale inverted confocal images. Scale bars: 200 µm.

**Supplemental Figure 3**

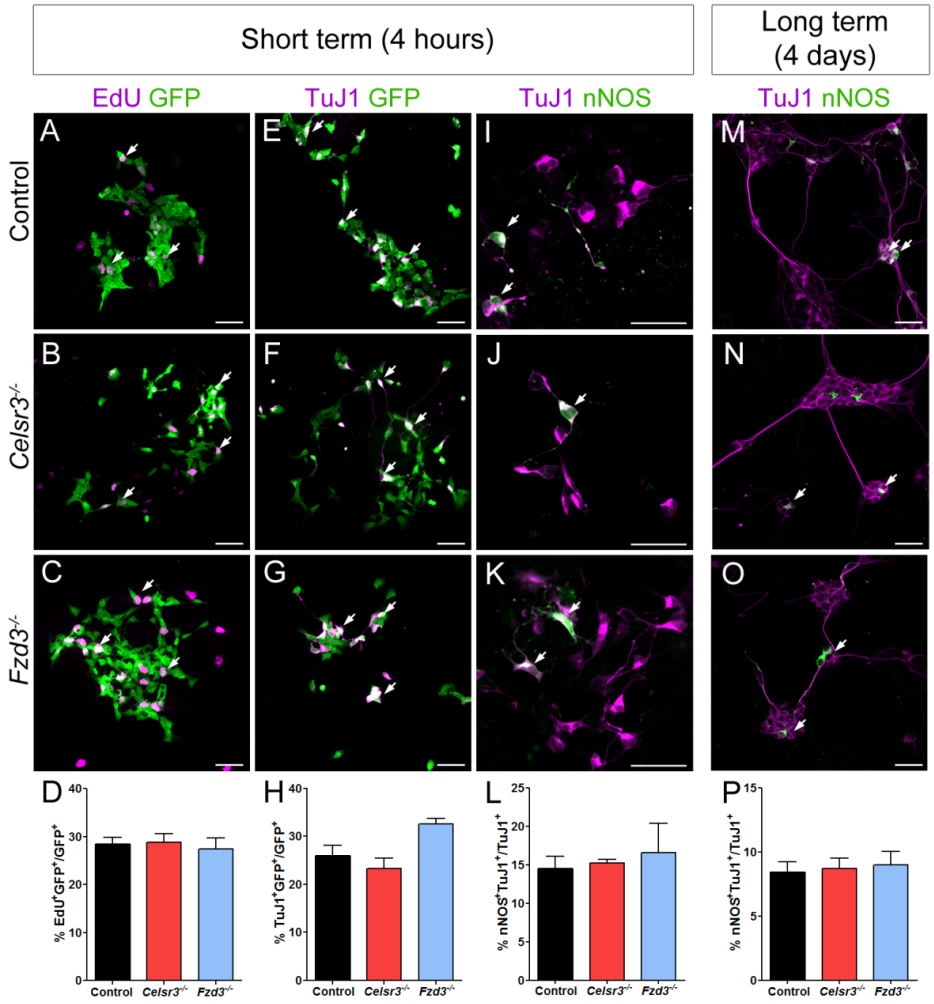


Proliferation and differentiation of enteric neural crest cells is unchanged in *Celsr3*- and *Fzd3*-deficient embryos. (**A** to **C**) EdU fluorescence (magenta) and GFP immunofluorescence (green) of short-term dissociated gut cultures from E12.5 control (A), Celsr3$^{-/-}$ (B) and *Fzd3*$^{-/-}$ (C) embryos transgenic for the *Wnt1-Cre;R26R-EYFP* reporter. Arrows point to double positive enteric neural crest cells. (**D**) Quantification of the EdU$^{+}$GFP$^{+}$ double positive cells among the neural crest derived cells of the gut (n ≥ 1400, N = 4, One-way ANOVA, ns) (**E** to **G**) TuJ1 (magenta) and GFP (green) immunofluorescence of short-term dissociated gut cultures from E12.5 control (E), *Celsr3*$^{-/-}$ (F) and *Fzd3*$^{-/-}$ (G) embryos transgenic for the *Wnt1-Cre;R26R-EYFP* reporter. Arrows point to double positive cells. (**H**) Quantification of the TuJ1$^{+}$GFP$^{+}$ double positive neurons among the neural crest derivatives of the gut (n ≥ 2000, One-way ANOVA, $P$ = 0.036; Bonferroni *post-hoc* vs Control, ns). (**I** to **K**) TuJ1 (magenta) and nNOS (green) immunofluorescence of short-term dissociated gut cultures from E12.5 control (I), *Celsr3*$^{-/-}$ (J) and *Fzd3*$^{-/-}$ (K) embryos. (**L**) Quantification of the nNOS$^{+}$TuJ1$^{+}$ double positive cells among all enteric neurons (n ≥ 650, One-way ANOVA, ns). (**M** to **O**) TuJ1 (magenta) and nNOS (green) immunofluorescence of long term cultures of primary neurons from E12.5 control (M), *Celsr3*$^{-/-}$ (N) and *Fzd3*$^{-/-}$ (O) embryos. (**P**)

Quantification of the $nNOS^{+}TuJ1^{+}$ double positive cells among all enteric neurons cultured 4 days in vitro ($n \geq 1100$, One-way ANOVA, ns). Scale bars: 50 μm.

**Supplemental Figure 4**

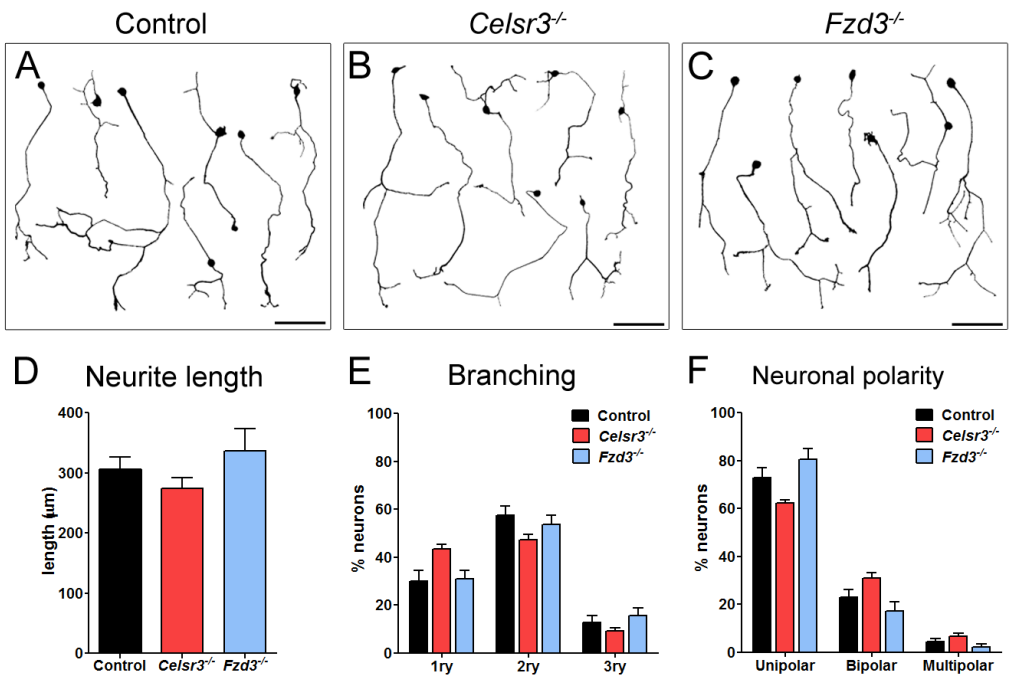


Deletion of *Celsr3* and *Fzd3* does not affect neuritogenesis of primary enteric neurons in culture. (**A** to **C**) Representative neurons immunostained for TuJ1 (black, grayscale inverted images) from cultures from control (A), *Celsr3*$^{-/-}$ (B) and *Fzd3*$^{-/-}$ (C) embryos. (**D**) Quantification of neurite length (One-way ANOVA, ns). (**E**) Quantification of branching pattern (One-way ANOVA, ns). (**F**) Quantification of neuronal polarity (unipolar and bipolar neurons, One-way ANOVA, $P < 0.05$; Bonferroni *post-hoc*, ns vs Control; multipolar, One-way ANOVA, ns). Differences between mutant and control neuronal cultures ($n \geq 220$, $N \geq 3$) were found to be not significant. Scale bars: 100 µm.

**Supplemental Figure 5**

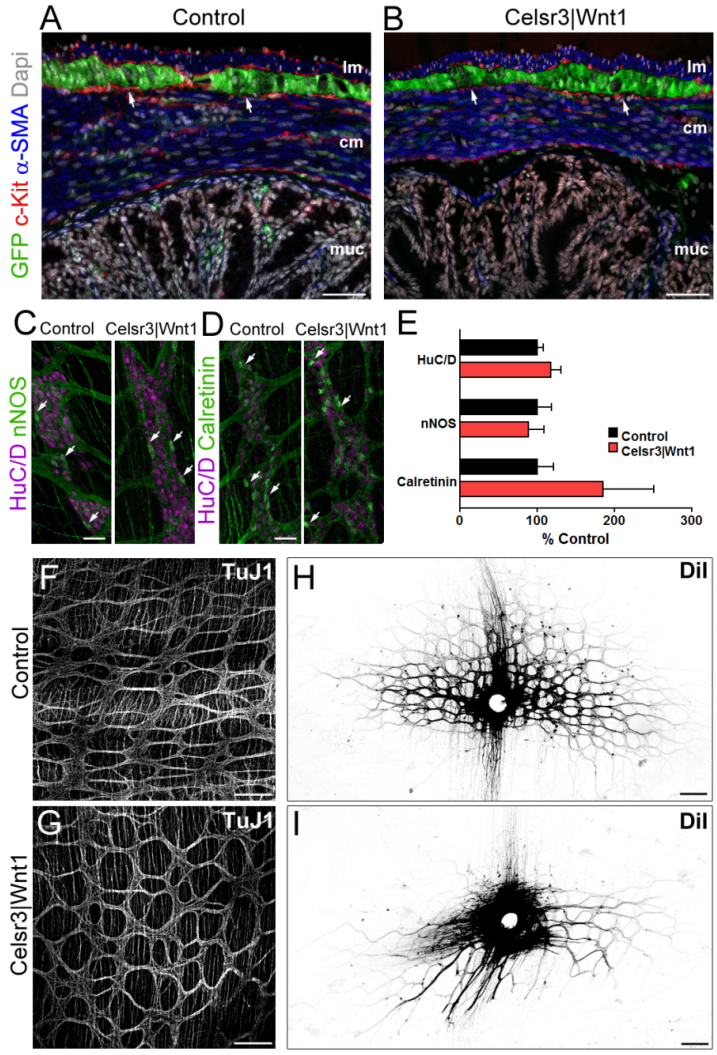


Specific effect of *Celsr3* inactivation on the organization of the myenteric plexus in the adult colon. (**A** and **B**) Gut cross sections immunostained with antibodies for GFP (green), c-Kit (red) α-smooth muscle actin (α-SMA, blue) and counterstained for DAPI (grey). (**C** and **D**) Myenteric ganglia immunostained for HuC/D (magenta) and nNOS (green, C) or calretinin (green, D). (**E**) Quantification of density of enteric neurons ($HuC/D^+$) per $mm^2$ and proportion of $nNOS^+$ and $calretinin^+$ neurons expressed as percentage of control ($n \geq 1300$, Student's *t*-test, ns). (**F** and **G**) Immunostaining for TuJ1 (grayscale). The organization of $TuJ1^+$ interganglionic strands in control preparations (F) is often changed in Celsr3|Wnt1 mutants (G). (**H** and **I**) DiI-labelling of myenteric plexus preparations shows a reduced number and length and the irregular pattern of fibers in mutants. Cm, circular muscle; lm, longitudinal muscle; muc, mucosa. Scale bars: 50 µm (A to D), 200 µm (F to I).

**Supplemental Figure 6**

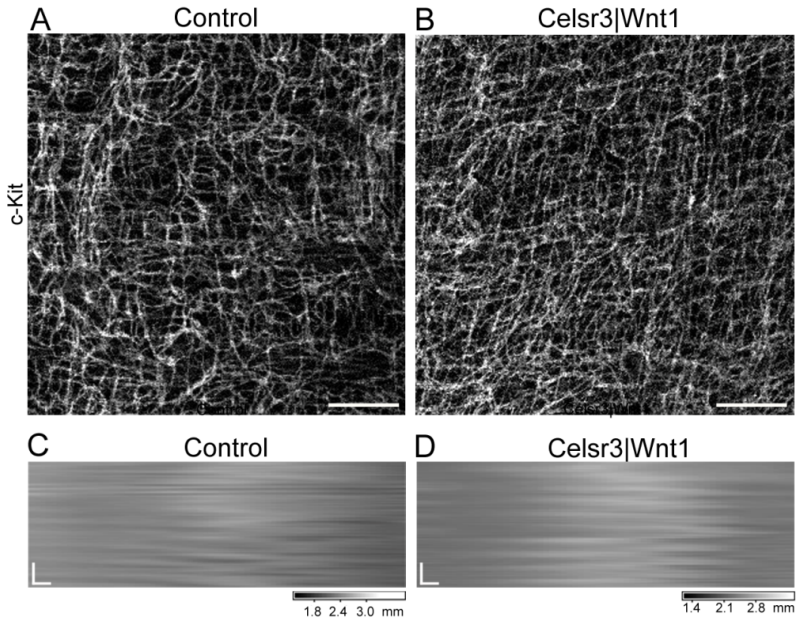


Normal network of interstitial cells of Cajal and generation of myogenic contractions in Celsr3|Wnt1 mice. (**A** and **B**) Confocal images of ileal longitudinal muscle and myenteric plexus preparations from control (A) and Celsr3|Wnt1 (B) mice immunostained for c-Kit (grayscale). No differences were observed in the density and arrangement of c-Kit$^{+}$ cells. Scale bars, 100 μm. (**C** and **D**) Video recordings of spontaneous motor patterns of colonic preparations from control (C) and Celsr3|Wnt1 (D) animals were analyzed using spatiotemporal maps. Maximal dilation (white), maximal constriction (black) and intermediate levels of constriction (grey scale) are represented over time (downwards). Myogenic contractions (also known as 'ripples') propagate for short distances in both oral and aboral directions and are undistinguishable between the two genotypes. Scale bars: 25 seconds (vertical) and 500 μm (horizontal).

**Legends to Supplemental Videos:**

**Supplemental Video 1.** Recording of spontaneous motor activity of an isolated colon from a wild-type mouse. The spatiotemporal map constructed from this original movie is shown in **Fig. 5C**. Movie is sped up 30 times.

**Supplemental Video 2.** Recording of spontaneous motor activity of an isolated colon from a Celsr3|Wnt1 mouse. The spatiotemporal map constructed from this original movie is shown in **Fig. 5D**. Movie is sped up 30 times.

**Supplemental Video 3.** Recording of motor activity upon insertion of an artificial pellet into the proximal colon of a wild-type mouse. The spatiotemporal map constructed from this original movie is shown in **Fig. 5K**. Movie is sped up 30 times.

**Supplemental Video 4.** Recording of motor activity upon insertion of an artificial pellet into the proximal colon of a Celsr3|Wnt1 mouse. The spatiotemporal map constructed from this original movie is shown in **Fig. 5L**. Movie is sped up 30 times.